Hydrostatic Stress Effect on the Optical Performance and the Stress Sensitivity of Optical Nonlinear Waveguide

تأثير الضغط الهيدروستاتيكي علي الأداء الضوئي وحساسية الضغط لمسلاك موجي ضوئي غير خطي

Hala El-Khozondar

هالة الخزندار

Department of Electrical and Computer Engineering.

Faculty of Engineering. Islamic University. Gaza. Palestine.

Email: hkhozondar@mail.iugaza.edu

Received: (19/2/2007). Accepted: (27/11/2007)

Abstract

Sensitivity of optical parameters is a significant topic in developing optoelectronic devices. The stress sensitivity of nonlinear optical waveguides is closely related to hydrostatic stress. The hydrostatic stress can cause anisotropic and inhomogeneous distribution of the refractive index. In this paper analytical and numerical calculations are performed to study the effect of hydrostatic stress on the sensitivity of nonlinear optical waveguide sensors. The optical performance of the waveguide sensors under various hydrostatic stress states is also investigated. Transverse magnetic modes (TM) are considered in addition to transverse electric modes (TE) to study anisotropy. It is found that the value of the hydrostatic stress can change the value of the cutoff thickness. These changes may induce multimode. Moreover, the hydrostatic stresses influence the values of the stress sensitivity of the waveguide sensors and present anisotropic behavior to the system.

ملخص

تعتبر حساسية العوامل الضوئية موضوعا مهما في تطوير الأجهزة الضوء إلكترونية. حساسية المسلاك الضوئي غير الخطي يمكن التحكم فيها بواسطة الضغط الهيدروستاتيكي. الضغط الهيدروستاتيكي يمكن أن يسبب توزيع غير خطي ومتباين لمعامل الانكسار الضوئي الفعلي للوسط. في هذا العمل تم إجراء حسابات تحليلية وعديدة لدراسة أثر الضغط الهيدروستاتيكي علي حساسية المَجَسّ الضوئي غير الخطي. تم دراسة الأداء الضوئي لِلمَجَسّ الضوئي تحت قيم مختلفة للضغط الهيدروستاتيكي. أُخِذَ في عين الاعتبار كل من الموجات الكهربائية المستعرضة (TE) والموجات المغناطيسية المستعرضة (TM). لقد وُجِد أن قيمة الضغط الهيدروستاتيكي تتحكم في قيمة سمك المسلاك الضوئي، الذي يحدد عدد الموجات المنتشرة (modes). إضافة إلي ذلك، فإن الضغط الهيدروستاتيكي يتحكم بحساسية المَجَسّ المسلاك الضوئي غير الخطي، وكذلك يسبب حدوث تباين في سلوك النظام.

1. Introduction

Waveguides can be constructed to carry waves over a wide portion of the electromagnetic spectrum, but are especially useful in the microwave and optical frequency ranges. Depending on the frequency, they can be constructed from either conductive or dielectric materials. Waveguides are used for transferring both power and communication signals. While perturbations are unfavorable in communications and power systems, they are welcomed in sensors (Ramo, S. & *et.al.* 19841).

In optical sensing, the response to external influence is intentionally enhanced so that the resulting change in optical radiation can be used as a measure of the external perturbation. Physical sensor based on the design and fabrication of a physical transducer capable of transform in an efficient way a chemical or biological reaction in a measurable signal [2]. Biochemical sensors are sensors which have been developed from slab structure with step index profile (Cush, R. & et.al. 1993). (Bernard, A. Bosshard, H. 1995).

The residual stresses due to fabrication and packing induce inhomogeneity and anisotropy on the behavior of the waveguide sensors by elasto-optic effect (Xu, J., Stroud, R. 1992). (Sapriel, J. 1979). Several studies have been performed to study the effect of elasto-optic effect on the optical performance of the waveguide (Saitoh, K. & et.al. 1999). (Huang,

M. 2003) has solved analytically the effect index and modes shape for a planar waveguides to illustrate the stress effect on the optical performance. El-Khozondar *et al.* (El-Khozondar, H. & et.al. 2007) has studied diverse stress values effect on the intensity of TE field propagating through nonlinear optical waveguide sensor. In the present paper, the responses of the dielectric constant of nonlinear optical waveguide sensor to hydrostatic stress states are analytically derived where TM fields are considered in addition to TE. Thus, birefringence can be investigated.

The wave equations of anisotropic and inhomogeneous waveguide will be derived in section 2. In section 3, the structure of the waveguide will be introduced. The focus of section 4 is on analytical calculation of the dispersion equation, the effective refractive index, and the effect of hydrostatic stress on the effective refractive index for both TE and TM fields. Section 5 studies the anisotropic behavior of the sensor while section 6 is dedicated to perform analytical calculation to determine the stress sensitivity of the effective refractive index with respect to external stress. The conclusion is presented in section ٧.

2. Wave equations of anisotropic and inhomogeneous waveguides

The electric filed E and the magnetic field H in a region containing no source are descried by the well known Maxwell's equations. Applying the simple-harmonic time varying fields to the Maxwell's equations will yield

$$\nabla \times \vec{E} = -\mu j \omega H, \tag{1}$$

$$\nabla \times \vec{H} = j \varepsilon \omega \vec{E}, \tag{2}$$

where ω is the angular frequency.

The stresses are usually inhomogeneous and anisotropic in the waveguide. For this reason, the resulting refractive indices are also inhomogeneous and anisotropic. Considering the waveguide very long in one direction, z, the shear stresses in this direction can be ignored. Therefore, the dielectric tensor is

$$\varepsilon = \begin{pmatrix} n_{xx}^2 & n_{xy}^2 & 0 \\ n_{xy}^2 & n_{yy}^2 & 0 \\ 0 & 0 & n_{zz}^2 \end{pmatrix}, \tag{3}$$

where n_{xx}, n_{yy}, n_{zz}, and n_{xy} are the refractive indices. These indices are functions of x, y and z. Due to the photo-elastic effect, the refractive indices change with stress and strain (Huang, M. 2003). For cubic structure media, the relation between refractive index, n, and strain, γ, is available in (Xu, J., Stroud, R. 1992). (Sapriel, J. 1979). The refractive index change caused by stress varies in the range ± 0.01.

In order to solve equations (1) and (2), two special cases are considered. Case 1: Transverse electric field (TE) where E_z=0. Case 2: Transverse magnetic field (TM) where H_z=0. If the following transformations are applied,

$$E(x, y, z) = e(x, y)\exp(-jn_e kz), \tag{4}$$

$$H(x, y, z) = h(x, y)\exp(-jn_h kz), \tag{5}$$

where n_e and n_h are effective indexes for TE and TM modes respectively and k is the wave number , the wave equations in terms of TE fields and TM fields will be obtained.

3. Asymmetric nonlinear planar sensor

The structure considered is asymmetric three layer waveguide sensor as shown in Fig.1. The sensor consists of an inhomogeneous film (Core) as described in section 2. The film thickness (t) is on the order of magnitude of the wavelength. The refractive index of the film is higher than the refractive indices of the surrounding cladding and substrate. The substrate has linear dielectric constant with refractive index n_s and the cladding is made of nonlinear material with an intensity dependent refractive index. The dielectric function of the nonlinear medium (Kerr-type) which is a function of the electric field can be expressed as,

$$\varepsilon_{cl}=\varepsilon_{c0}+\alpha\left|E_y\right|^2, \tag{6}$$

where ε_{c0} is the linear relative permittivity and α is the nonlinear coefficient (Boardman, A. & Egan, P. 1986). (Khozondar, H. 2004). (Stegeman, G. & et.al. 1985). For planar waveguides, the light propagates in the z direction, is confined in the x direction within the central core, and has no variation in the y direction.

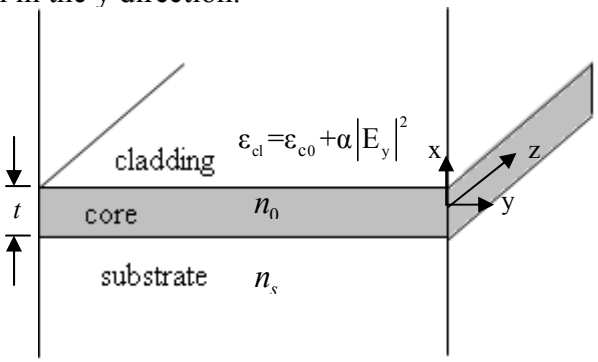

Figure (1): Schematic of asymmetric three layer planer waveguide.

In this paper, TE and TM fields are investigated. For TE fields using equations (1) and (2) and E_z=0, the mode equation for the core region, $-t/2 \le x \le t/2$, can be written as,

$$\frac{d^2 e_y}{dx^2}+k^2\left(n_{yy}^2-n_e^2-\frac{n_{xy}^2}{n_{xx}^2-n_e^2}\right)e_y=0 \tag{7}$$

For the clad region, $x \ge t/2$, the mode equation is derived as follows,

$$\frac{d^2 e_y}{dx^2}+k^2\left(\varepsilon_{c0}-n_e^2\right)e_y+\alpha k^2\left|e_y^2\right|e_y=0, \tag{8}$$

Similarly, for the dielectric substrate, $x \le -t/2$, the mode equation will be expressed as,

$$\frac{d^2 e_y}{dx^2} - k^2\left(n_e^2 - n_s^2\right)e_y = 0 \tag{9}$$

Also for TM fields, applying equations (1) and (2) and H_z=0, the mode equation for the core region,-t/2≤x ≤t/2, can be written as,

$$\frac{d^2 h_y}{dx^2} + p\frac{dh_y}{dx} + k^2\frac{n_{zz}^2}{n_{xx}^2}\left(n_{xx}^2 - n_h^2 - \frac{n_{xy}^2}{n_{yy}^2 - n_e^2}\right)h_y = 0, \tag{10}$$

where $p(x) = \frac{-2}{n_{zz}}\frac{dn_{zz}}{dx}$.

For the clad region, x ≥t/2, the mode equation is obtained as follows,

$$\frac{d^2 h_y}{dx^2} + k^2\left(\varepsilon_{c0} - n_h^2\right)h_y + \alpha k^2\left|h_y^2\right|h_y = 0, \tag{11}$$

And similarly for the dielectric substrate, x ≤-t/2, the mode equation will be given by,

$$\frac{d^2 h_y}{dx^2} - k^2\left(n_h^2 - n_s^2\right)h_y = 0 \tag{12}$$

Solving the above equations produces TE and TM modes. To consider the stress effects, in the next discussion, hydrostatic stress is applied assuming infinite thick cladding and substrate regions. To emphasize the stress effects on the core and to simplify the calculations, the photoelastic effects of the cladding and substrate regions are ignored.

4. Hydrostatic stress state

Core is assumed to be under hydrostatic state, *i.e.*, $\sigma_{xx}= \sigma_{yy}=\sigma_{zz}=\sigma$ and σ_{xy} =0. Therefore, the index of the core is isotropic and homogenous, and the changes due to stress, *i.e.*, $n_{xx}=n_{yy}=n_{zz}=n=n_0-(C_1+2C_2)\sigma$ and n_{xy}=0. In this section, the effect of hydrostatic stress effect on the nonlinear sensor is studied for both TE and TM modes.

4. 1. TE Modes

TE mode is considered when the electric field component in the propagation direction is equal to 0, Ez=0. This will simplify the modes equations in the three layers. The mode equation relating to the core, $-t/2 \leq x \leq t/2$, is

$$\frac{d^2 e_y}{dx^2} + k^2 (n^2 - n_e^2) e_y = 0 \tag{13}$$

The solution of equation (13) is

$$e_y = B_e \cos\left(kx\sqrt{n^2 - n_e^2}\right) + C_e \sin\left(kx\sqrt{n^2 - n_e^2}\right). \tag{14}$$

For the substrate region, $x \leq -t/2$, the solution of equation (9) is

$$e_y = D_e \exp\left(kx\sqrt{n_e^2 - n_s^2}\right) \tag{15}$$

The solution of equation (8) for the nonlinear cladding, $x \geq t/2$, is

$$e_y = A_e \frac{q_c}{\sqrt{\Lambda}} \operatorname{sech}\left(q_c\left(x - x_0\right)\right), \tag{16}$$

where $q_c = k\sqrt{n_e^2 - \varepsilon_0}, \Lambda = \frac{k^2}{2}\alpha,$ and x_0 is a constant of integration at maximum power (Boardman, A. & Egan, P. 1986). (Khozondar, H. 2004). (Stegeman, G. & et.al. 1985). In the above solutions, it has been taken into account that fields approach zero at large values of x. The constants A_e, B_e, C_e, and D_e are calculated from the boundary conditions.

At the interface between core-substrate and core-cladding, e_y and $h_z \sim de_y/dx$ are continuous across the boundary (Boyd, J. 1994). Applying these boundary conditions produce four homogeneous linear equations. For these equations to have nontrivial solution for the constants, the determinant of the coefficient must be equated to zero. This results in the following dispersion equations

$$\tan p_e = \left(\beta_e + \sqrt{\beta_e^2 + 1}\right); \quad \text{even modes}$$
$$\tan p_e = \left(\beta_e - \sqrt{\beta_e^2 + 1}\right); \quad \text{odd modes} \tag{17}$$

where

$$p_e = \frac{kt}{2}\sqrt{n^2 - n_e^2}\,,\ \beta_e = \tan\left(\kappa_{e1} - \kappa_{e2}\right),\ \tan\left(\kappa_{e1}\right) = \sqrt{\frac{n_e^2 - n_s^2}{n^2 - n_e^2}},$$

$$\tan\left(\kappa_{e2}\right) = \frac{k\sqrt{n^2 - n_e^2}}{\eta},$$

and $\eta = q_c \tanh\left(q_c\left(\frac{t}{2} - x_0\right)\right)$.

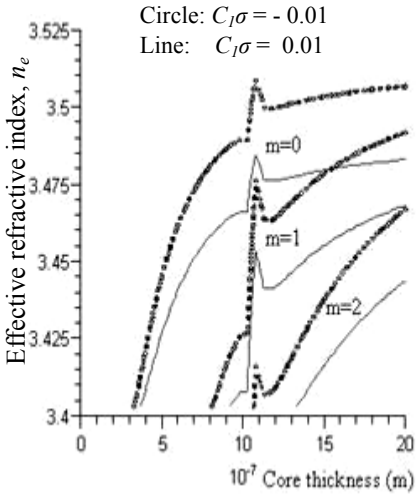

Figure (2): Effective refractive index, n_e, versus the core thickness for the first TE modes in the asymmetric planar optical waveguide under different hydrostatic stresses.

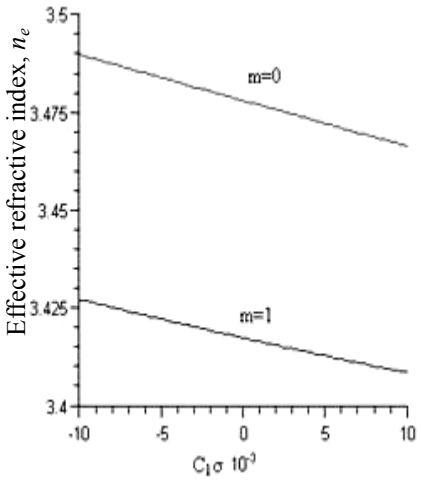

Figure (3): Effective refractive index, n_e, for the first TE modes versus the normalized hydrostatic stress for asymmetric planar optical waveguide with thickness t=1μm

The refractive index is drawn in Fig. 2 as a function of the core thickness for the first three modes (m=0, 1, and 2). Fig. 3 exhibits the effective refractive index as a function of hydrostatic stress for asymmetric planar waveguide with the core thickness has the value, t=1μm. As shown in Fig. 2 and Fig. 3, the numbers of modes vary with the values of the hydrostatic stress and the thickness of the core. The core with t = 1 μm allows only the first two modes to propagate. In Fig. 2, higher order modes will appear at t > 1 μm. The cutoff thickness can be controlled by varying the stress values. For example, when $C_1\sigma = 0.01$, only zero mode will propagate at cutoff thickness less than 0.9 μm. For $C_1\sigma = -0.01$ the cutoff thickness will change to a value less than 0.8 μm.

4.2. TM modes

TM mode is considered when the magnetic field component in the direction of propagation is equal to zero, Hz=0. The mode equation (10) of the core, $-t/2 \le x \le t/2$, will be simplified to

$$\frac{d^2 h_y}{dx^2} + k^2 (n^2 - n_h^2) h_y = 0, \tag{18}$$

and its solution is

$$h_y = B_h \cos\left(kx\sqrt{n^2 - n_h^2}\right) + C_h \sin\left(kx\sqrt{n^2 - n_h^2}\right) \tag{19}$$

The solution of equation (12), in the substrate region, $x \le -t/2$, can be written as,

$$h_y = D_h \exp\left(kx\sqrt{n_h^2 - n_s^2}\right) \tag{20}$$

In the nonlinear cladding region, $x \ge t/2$, the solution of equation (11) will be

$$h_y = A_h \frac{q_c}{\sqrt{\Lambda}} \operatorname{sech}\left(q_c\left(x - x_0\right)\right), \tag{21}$$

where q_c, Λ and x_0 are defined earlier. The boundary conditions of zero fields at large values of x are considered in equations (19, 20, and 21). A_h, B_h, C_h, and D_h are constants. At the interface between core and cladding, the boundary conditions are the continuity of h_y and $e_z \sim n^{-2} dh_y/dx$ across the boundary (Boyd, J. 1994). Applying similar procedure to TE mode results in the following dispersion equations

$$\begin{aligned} &\tan p_h = \left(\beta_h + \sqrt{\beta_h^2 + 1}\right); \quad \text{even modes} \\ &\tan p_h = \left(\beta_h - \sqrt{\beta_h^2 + 1}\right); \quad \text{odd modes} \\ &\tan p = \left(\beta + \sqrt{\beta^2 + 1}\right), \text{ for even modes} \\ &\tan p = \left(\beta + \sqrt{\beta^2 + 1}\right), \text{ for odd modes} \end{aligned} \tag{22}$$

where

$$p_h = \frac{kt}{2}\sqrt{n^2 - n_h^2}\ , \beta_h = \tan\left(\kappa_{h1} - \kappa_{h2}\right), \tan\left(\kappa_{h1}\right) = \frac{n^2}{n_c^2 n_s^2}\sqrt{\frac{n_h^2 - n_s^2}{n^2 - n_h^2}},$$

$$\tan\left(\kappa_{h2}\right) = \frac{k\sqrt{n^2 - n_h^2}}{n^2 \eta}, \text{ and } \eta = q_c \tanh\left(q_c\left(\frac{t}{2} - x_0\right)\right).$$

Fig. 4 shows the refractive index for the first three TM modes as a function of the core thickness. The number of modes is controlled by changing the thickness of the film. The effective refractive index is plotted as a function of hydrostatic stress with t=1μm in Fig. 5. It shows that the number of modes can be controlled by changing the value of the hydrostatic stress. When stress values change, the second mode (m=2) appear or disappear.

In all the calculations, the values of the optical parameters are: n_0=3.5, n_1=3.4, ε_0=2.7, $\alpha=10^{-9}$ m^2/W, λ=0.83μm, and C_1/C_2=0.1.

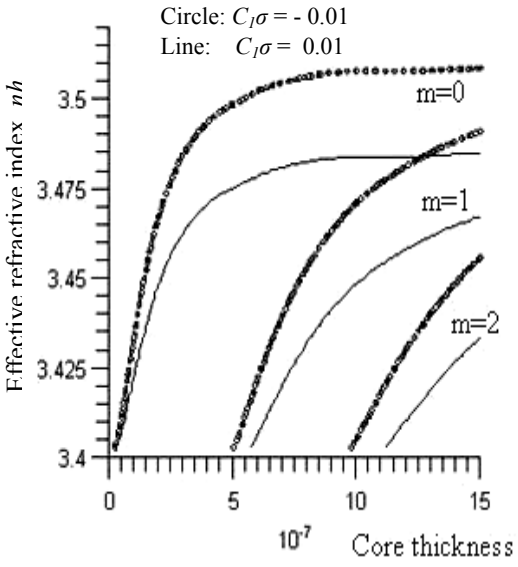

Figure (4): Effective refractive index, n_h, versus the core thickness for the first TM modes in the asymmetric planar optical waveguide under different hydrostatic stresses**.**

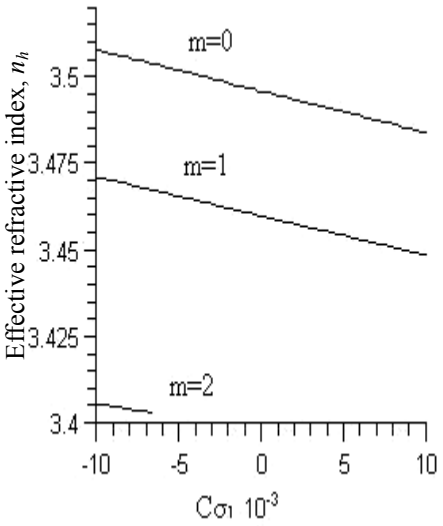

Figure (5): Effective refractive index, n_h, for the first TM modes versus the normalized hydrostatic stress for asymmetric planar optical waveguide with thickness t=1μm.

5. Optical Anisotropy

Birefringence phenomenon occurs when an isotropic material is subjected to mechanical stress, it becomes anisotropic. This phenomenon is known as optical anisotropy. Polarization Shift (PS) is used to describe the wavelength difference between TE and TM mode which can be determined as follows

$$PS = \lambda_{TE} - \lambda_{TM} = (n_e - n_h)\lambda \qquad (23)$$

Fig. 6 shows the discrepancies between the effective index of TE and TM modes at different stress values. This difference between the values of effective refractive indices for both TE and TM modes causes anisotropic behavior of the waveguide sensor. Therefore, the two polarization modes propagate at different speeds.

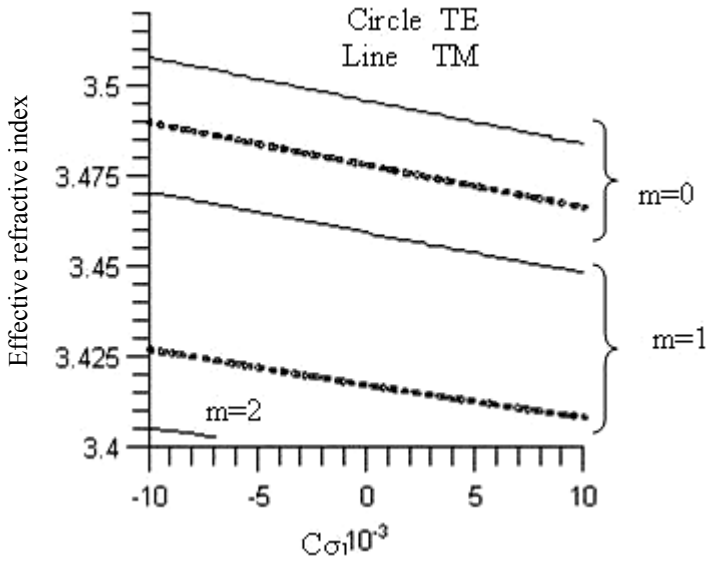

Figure (6): Effective refractive indexes, n_e and n_h, for TE and TM modes versus the core thickness for asymmetric planar optical waveguide under different hydrostatic stresses.

6. Stress sensitivity of the effective refractive index

Stress sensitivity of effective refractive index of nonlinear optical waveguides under changeable hydrostatic stress is the rate of change of effective refractive index with respect to stress, $dn_i/d\sigma$. The stress sensitivity is calculated by Differentiating equation (17) for TE and equation (22) for TM with respect to stress, σ. The stress sensitivity of effective refractive index of the even and odd modes has identical shape as

$$\sec^2(p_i)\frac{dp_i}{d\sigma} = \frac{\beta_i + \sqrt{\beta_i^2 + 1}}{\sqrt{\beta_i^2 + 1}}\frac{d\beta_i}{d\sigma} \tag{24}$$

where *i* stands for e (TE mode) and h (TM mode).

In Fig. 7, the stress sensitivity, $dn_e/d\sigma$, is plotted as a function of the core thickness for the zero mode TE fields. The stress sensitivity varies with the core thickness and is sensitive to different stress values. The stress sensitivity for zero mode TM field, $dn_h/d\sigma$, as function of core thickness is demonstrated in Fig.8. The stress sensitivity changes for different stress values as a function of core thickness. The values used in the calculation for the variation of effective indices with respect to stress, σ, are: $\partial n/\partial\sigma$ =-1.2E-11, $\partial n_1/\partial\sigma$ =-1E-11, and $\partial\varepsilon_0/\partial\sigma$ = 2E-11. Unit is Pa^{-1}.

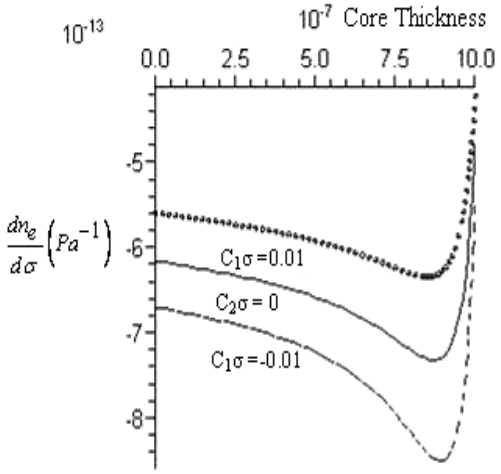

Figure (7): Stress sensitivity of the effective refractive index as a function of core thickness for different stress state for zero mode TE field.

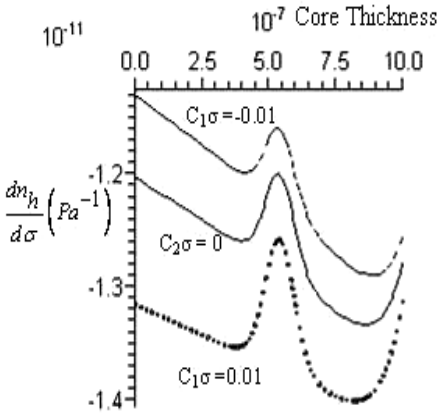

Figure (8): Stress sensitivity of the effective refractive index as a function of core thickness for different stress state for zero mode TM field.

7. Conclusion

Through fabrication of the waveguide sensors, induced stresses can cause changes in the effective refractive index of the waveguide. The hydrostatic stress effect on the effective refractive index is numerically calculated. It is found that hydrostatic stress causes small changes in the value of refractive indices resulting in an unacceptable optical performance, such as, multimode and anisotropy. Thus, elasto-optics effect is used to compensate the stress effects of the nonlinear optical waveguide sensors. The stress sensitivity of the effective refractive index has a direct relationship with hydrostatic stress for both TE and TM of the waveguide sensors. Therefore, the hydrostatic stress states can be used to control the stress sensitivity of the effective refractive index. As a result, the stress sensitivity of the effective refractive index can be carefully tuned considering the size of the sensor. Consequently, the number of modes can be controlled by changing the size of the sensor.

References

- Ramo, S. Whinnery, J. R. & van Duzer, T. (1984). Fields and Waves in Communications Electronics. 2ed. John Wiley and Sons. New York. U.S.A.
- Ghatak, A. & Thyagarajan, K. (1998). Introduction to Fiber Optics. University Press. Cambridge. U.K.
- Cush, R. Cronin, J. Stewart, W. Maule, C. Molloy, J. & Goddard, N. (1993). "The resonant mirror: A novel optical biosensor for direct sensing of bio-molecular interactions". Part I: Principle of operation and associated instrumentation, Biosensors Bioelectron. (8). 347-353.
- Bernard, A. Bosshard, H. (1995). "Real-time monitoring of antigen-antibody recognition on a metal oxide surface by an optical grating coupler sensor". European J. Biochem. (230). 416-423.
- Xu, J. Stroud, R. (1992). Acousto-optic Devices: Principles, Design, and Applications. John Wiley and Sons. New York. U.S.A.
- Sapriel, J. (1979). Acosto-optics. John Wiley and Sons. New York. U.S.A.
- Saitoh, K. Koshiba, M. Tsuji, Y. (1999). "Stress analysis method for elastically anisotropic material based optical waveguides and its application to strain-induced optical waveguides". Journal of Lightwave Technology (17). 255-259.
- Huang, M. (2003). "Stress effect on performance of optical waveguides". International Journal of Solids and Structures (40). 1615-1632.
- El-Khozondar, H. El-Khozondar, R. Shabat, M. & Kock, A. (2007). "Stress effect on optical nonlinear waveguide sensor". J. Optical communication. in press.
- Boardman, A. & Egan, P. (1986). "Optically nonlinear waves in thin films". IEEE of quantum electronics QE. 22 (2). 319-324.

- Khozondar, H. Saifi, R. Shabat, M. M. (2004). "Nonlinear surface wave guided by a single periodic medium". Laser Physics 14 (12).1539-1543.
- Stegeman, G. Seaton, C.T. Ariyasu, J. Wallis, R. Maradudin, A. (1985). "Nonlinear electromagnetic waves guided by a single interface". J. Appl. Phys. 58 (7). 2453-2459.
- Boyd, J. (1994). "Photonic integrated circuits". In: R. G. Hunsperger. Photonic Devices and Systems. Marcel Dekker. New York.U.S.A.
- Adams, M. (1981). An Introduction to Optical Waveguide. John Wiley and Sons. Chichester.
- Parriaux, O. & Veldhuis, G. J. (1998). "Normalized Analysis for Sensitivity Optimization of Integrated Optical Evanescent-Wave Sensors". J. Lightwave Tech. (16). 573-582.